

# Hunting scalar leptoquarks with boosted tops in pair and single production channels

Kushagra Chandak,<sup>1,\*</sup> Tanumoy Mandal,<sup>2,†</sup> and Subhadip Mitra<sup>1,‡</sup>

<sup>1</sup>Center for Computational Natural Sciences and Bioinformatics,  
International Institute of Information Technology, Hyderabad 500 032, India

<sup>2</sup>Department of Physics and Astronomy, Uppsala University, Box 516, SE-751 20 Uppsala, Sweden  
(Dated: March 9, 2022)

The LHC search strategies for leptoquarks that couple dominantly to the top quark are different than the ones that couple mostly to light quarks. We consider TeV-scale charge  $1/3$  ( $\phi_1$ ) and  $5/3$  ( $\phi_5$ ) scalar leptoquarks that can decay to a top quark and a charged lepton pair ( $t\ell$ ) giving rise to a resonance system with a boosted top quark and a high- $p_T$  lepton at the LHC. We implement a search strategy for these leptoquarks with a signal that is a combination of pair and single production channels by selecting events with at least one hadronically decaying boosted top and two high- $p_T$  same flavour opposite sign leptons. While the pair production is best for discovery in the lower mass region, our combined signal can substantially improve the LHC discovery reach as single productions generally overcome pair production in the high mass region. Contrary to the general consensus, we find that the single production of top-philic  $\phi = \{\phi_1, \phi_5\}$  in association with a lepton and jets could be significant for order one  $\phi t\ell$  coupling if  $\phi$  couples to a left-handed top quark. Our estimate shows that the leptoquark searches in the  $t\ell\ell + X$  channel can discover a scalar leptoquark as heavy as 2.1 TeV with  $5\sigma$  significance for some coupling configurations at the 14 TeV HL-LHC.

## I. INTRODUCTION

So far, the predictions of the Standard Model (SM) of particle physics have been verified to a remarkable degree of accuracy. But some persistent deviations in the rare  $B$ -meson decays observed in several experiments indirectly hint towards new physics. In particular, an excess in the  $R_{D^{(*)}}$  observables was first reported by the BaBar collaboration in 2012 [1, 2]. Till now, this excess has survived the LHCb [3–5] and Belle [6–8] measurements. The current combined deviation in the  $R_D$  and  $R_{D^*}$  observables, as computed by the HFLAV group [9], is still about  $3.1\sigma$  away from the SM prediction [10–13]. A significant suppression of about  $2.5\sigma$  in the  $R_{K^{(*)}}$  observables from their SM predictions [14, 15] have been observed by the LHCb collaboration [16–20]. Altogether, a common feature of these deviations indicate towards lepton universality violation and suggests the underlying new physics, if that really is the origin of these anomalies, has strong affinity towards the third generation SM fermions.

A possible explanation of the rare  $B$ -decay anomalies is the existence of TeV-scale scalar leptoquarks (LQ or  $\ell_q$ ) that has large couplings to the third generation quarks. LQs appear in different BSM scenarios like Pati-Salam models [21], SU(5) grand unified theories [22], the models with quark lepton compositeness [23],  $R$ -parity violating supersymmetric models [24] or coloured Zee-Babu model [25] etc. Their phenomenology has also been studied in great detail (see, for example, Refs. [26–30] for some phenomenological studies).

The LHC is actively looking for signatures of LQs for some time and has put direct detection bounds on ones that couple with third generation fermions. Assuming  $Br(\ell_q \rightarrow t\tau) = 1$ , a recent scalar LQ pair production search at the CMS detector has excluded masses below 900 GeV [31]. CMS has also put bounds on scalar LQs that decay to a  $b$ -quark and a neutrino at about 1.1 TeV assuming 100% branching ratio (BR) in this decay mode [32]. Some of the limits are also available from the ATLAS searches [33, 34].

Generally, though studies on LQs that couple to quarks and leptons of same generation are mostly found in the literature, it is possible to have LQs with large cross-generation couplings i.e. a LQ that couples to quarks and leptons of different generations [35, 36]. However, large cross-generational couplings might introduce FCNC which is strongly constrained from precision experiments. These bounds are not strong when LQs have couplings with third generation fermions. Note that since LQs carry lepton numbers, scenarios with comparable couplings of a LQ to leptons of different generations simultaneously (and hence comparable BRs to those modes) are possibly constrained from the lepton number/flavour violation searches. In this paper, we focus on the scalar LQs that decay to a top quark and a charged light lepton (either electron or muon). With this, pair production of such LQs would have either of the two possible signatures viz.  $t\ell\mu\mu$  and  $t\ell ee$ . Among them  $t\ell\tau\tau$  mode is already extensively searched for by the ATLAS and the CMS collaborations. CMS has recently published their first analysis of LQ pair production searches in the  $t\ell\mu\mu$  channel [37]. A prospect study at the HL-LHC for this channel has also been performed by the CMS collaboration [38].

In this paper, we implement a combined search strategy [39–41] by putting events from pair and single productions of scalar LQs together to enhance their discovery potential/reach at the 14 TeV HL-LHC. Here, our aim is to use a dedicated top-tagger with good tagging efficiency to tag hadronically decaying boosted top quarks in the final states to estimate the LHC discovery potential of LQs in the  $t\ell\ell + X$  (where  $\ell = \{e, \mu\}$ ) mode. Motivated by the  $B$ -decay anomalies, we investigate the effects of large cross-generational LQ-quark-lepton Yukawa couplings on the direct discovery potential of HL-LHC. We find that depending on the coupling configurations, the single productions ( $pp \rightarrow \ell_q \ell j + \ell_q \ell t$ ) could be comparable to the pair production and even bigger in the high mass region. This is in contrast to the common expectation that LQs that couples with third generation quarks would have small single production cross sections.

The rest of the paper is organized as follows. In Section II, we introduce the leptoquark models. In Section III we discuss LHC phenomenology of the scalar leptoquarks, our search strategy and present our results and finally in Section IV we conclude.

\* kushagra.chandak@research.iiit.ac.in

† tanumoy.mandal@physics.uu.se

‡ subhadip.mitra@iiit.ac.in

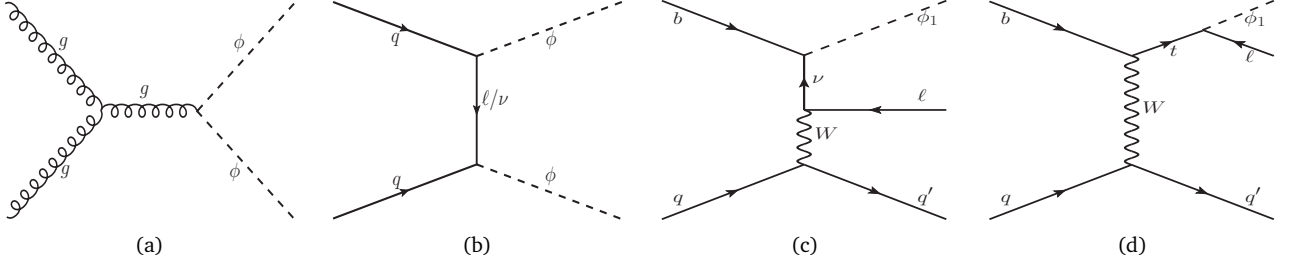


FIG. 1. Sample Feynman diagrams for LQ production at the LHC. Diagrams (a) and (b) show pair production processes and (c) and (d) are examples of single productions.

## II. LEPTOQUARK MODELS

As mentioned, we are interested in top-philic scalar LQs that decay substantially to a top quark and an electron or a muon. Electromagnetic charge conservation requires such a LQ must have electromagnetic charge  $\pm 1/3$  or  $\pm 5/3$ . From the classifications of possible LQ states in Refs. [42, 43] we see that only  $S_1$ ,  $R_2$  and  $S_3$  have the desired decay modes  $\ell_q \rightarrow t\ell$  (where  $\ell = \{e, \mu\}$ ). Below, we show these three types of LQs Lagrangians following the notations of Ref. [43]. To avoid proton decay constraints we ignore the diquark operators.

$S_1 = (\bar{3}, 1, 1/3)$ :

For  $S_1$ , one can write the following two renormalizable operators invariant under the SM gauge group ( $G_{\text{SM}}$ ):

$$\mathcal{L} \supset y_{1ij}^{LL} \bar{Q}_L^C i S_1 \tau^2 L_L^j + y_{1ij}^{RR} \bar{u}_R^C i S_1 e_R^j + \text{h.c.}, \quad (1)$$

where  $Q_L$  and  $L_L$  are the SM left-handed quark and lepton doublets, respectively. The superscript  $C$  in  $Q_L^C$  denotes charge conjugation. The Pauli matrices are represented by  $\tau^k$  with  $k = \{1, 2, 3\}$ . Here, the generation indices are denoted by  $i, j = \{1, 2, 3\}$ . This can be written explicitly as,

$$\mathcal{L} \supset - (y_{1ij}^{LL} U)_{ij} \bar{d}_L^C i S_1 \nu_L^j + (V^T y_{1ij}^{LL})_{ij} \bar{u}_L^C i S_1 e_L^j + y_{1ij}^{RR} \bar{u}_R^C i S_1 e_R^j + \text{h.c.}, \quad (2)$$

where  $U$  and  $V$  represent the neutrino mixing or the Pontecorvo-Maki-Nakagawa-Sakata (PMNS) matrix and the Cabibbo-Kobayashi-Maskawa (CKM) or the quark mixing matrix, respectively. Since the neutrino flavours cannot be distinguished at the LHC, we ignore the flavour of the neutrinos and denote them by just  $\nu$ . Similarly, for LHC phenomenology in general and, in particular, our analysis, the small off-diagonal terms of the CKM matrix play negligible role. Hence, for simplicity, we assume a diagonal CKM matrix. We can now identify the terms relevant for our analysis,

$$\mathcal{L} \supset y_{13j}^{LL} \left( -\bar{b}_L^C \nu_L + \bar{t}_L^C \ell_L^j \right) S_1 + y_{13j}^{RR} \bar{t}_R^C \ell_R^j S_1 + \text{h.c.}, \quad (3)$$

where  $j = \{1, 2\}$  now.

$S_3 = (\bar{3}, 3, 1/3)$ :

There is only one type of  $G_{\text{SM}}$ -invariant renormalizable operator one can write for  $S_3$ :

$$\mathcal{L} \supset y_{3ij}^{LL} \bar{Q}_L^C i, a \epsilon^{ab} (\tau^k S_3^k)^{bc} L_L^{j,c} + \text{h.c.}, \quad (4)$$

Here, the SU(2) indices are denoted by  $a, b, c = \{1, 2\}$ .

$$\begin{aligned} \mathcal{L} \supset & - (y_{3ij}^{LL} U)_{ij} \bar{d}_L^C i S_3^{1/3} \nu_L^j - \sqrt{2} y_{3ij}^{LL} \bar{d}_L^C i S_3^{4/3} e_L^j \\ & + \sqrt{2} (V^T y_{3ij}^{LL} U)_{ij} \bar{u}_L^C i S_3^{-2/3} \nu_L^j \\ & - (V^T y_{3ij}^{LL})_{ij} \bar{u}_L^C i S_3^{1/3} e_L^j + \text{h.c.}, \end{aligned} \quad (5)$$

The terms relevant for us are,

$$\begin{aligned} \mathcal{L} \supset & - y_{33j}^{LL} \left[ \left( \bar{b}_L^C \nu_L + \bar{t}_L^C \ell_L^j \right) S_1^{1/3} + \sqrt{2} \left( \bar{b}_L^C \ell_L^j S_3^{4/3} \right. \right. \\ & \left. \left. - \bar{t}_L^C \nu_L S_3^{-2/3} \right) \right] + \text{h.c.}, \end{aligned} \quad (6)$$

with  $j = \{1, 2\}$ .

$R_2 = (3, 2, 7/6)$ :

Similarly for  $R_2$  one gets,

$$\begin{aligned} \mathcal{L} \supset & - y_{2ij}^{RL} \bar{u}_R^i R_2^a \epsilon^{ab} L_L^{j,b} + y_{2ji}^{LR} \bar{e}_R^j R_2^{a*} Q_L^{i,a} + \text{h.c.} \\ \text{or, } \mathcal{L} \supset & - y_{2ij}^{RL} \bar{u}_R^i e_L^j R_2^{5/3} + (y_2^{RL} U)_{ij} \bar{u}_R^i \nu_L^j R_2^{2/3} \\ & + (y_2^{LR} V^\dagger)_{ji} \bar{e}_R^j u_L^i R_2^{5/3*} + y_{2ji}^{LR} \bar{e}_R^j d_L^i R_2^{2/3*} \\ & + \text{h.c.} \end{aligned} \quad (7)$$

We identify the terms relevant for us,

$$\begin{aligned} \mathcal{L} \supset & - y_{23j}^{RL} \bar{t}_R \ell_L^j R_2^{5/3} + y_{23j}^{RL} \bar{t}_R \nu_L R_2^{2/3} \\ & + y_{2j3}^{LR} \bar{\ell}_R^j t_L R_2^{5/3*} + y_{2j3}^{LR} \bar{\ell}_R^j b_L R_2^{2/3*} + \text{h.c.}, \end{aligned} \quad (8)$$

with  $j = \{1, 2\}$ .

### A. Simplified Model and Benchmark Scenarios

Following Ref. [40], we can write a simplified effective phenomenological Lagrangian from the above equations,

$$\mathcal{L} \supset \lambda_\ell \left( \sqrt{\eta_L} \bar{t}_L^C \ell_L + \sqrt{\eta_R} \bar{t}_R^C \ell_R \right) \phi_1 + \lambda_\nu \bar{b}_L^C \nu_L \phi_1 + \text{h.c.}, \quad (9)$$

$$\mathcal{L} \supset \tilde{\lambda}_\ell \left( \sqrt{\eta_L} \bar{t}_R \ell_L + \sqrt{\eta_R} \bar{t}_L \ell_R \right) \phi_5 + \text{h.c.} \quad (10)$$

In this notation, a charge 1/3 (5/3) scalar LQ is generically represented by  $\phi_1$  ( $\phi_5$ ). Like in Ref. [40],  $\eta_L$  and  $\eta_R = (1 - \eta_L)$  are the fractions of lepton coming from a LQ decay that are left-handed and right-handed, respectively. Note that the simplified Lagrangian does not include any charge 2/3 or 4/3 LQ as such LQs would not couple with a top quark and a charged lepton simultaneously at the tree level.

For our analysis, we consider four benchmark coupling scenarios.

Benchmark scenario	Possible charge(s)	Simplified model [Eqs. (9) – (10)]			LQ models [Eqs. (3) – (8)]		Decay mode(s)	Branching ratio(s)
		Type of LQ	Non-zero couplings equal to $\lambda$	Lepton chirality fraction	Type of LQ	Non-zero coupling equal to $\lambda$		
LCSS	1/3	$\phi_1$	$\lambda_\ell = \lambda_\nu$	$\eta_L = 1, \eta_R = 0$	$S_3^{1/3}$	$-y_{3\ 3j}^{LL}$	$\{t\ell, b\nu\}$	$\{50\%, 50\%\}$
LCOS	1/3	$\phi_1$	$\lambda_\ell = -\lambda_\nu$	$\eta_L = 1, \eta_R = 0$	$S_1$	$y_{1\ 3j}^{LL}$	$\{t\ell, b\nu\}$	$\{50\%, 50\%\}$
RC	1/3, 5/3	$\phi_1, \phi_5$	$\tilde{\lambda}_\ell, \lambda_\ell$	$\eta_L = 0, \eta_R = 1$	$S_1, R_2^{5/3}$	$y_{1\ 3j}^{RR}, y_{2\ j3}^{LR}$	$t\ell$	100%
LC	5/3	$\phi_5$	$\tilde{\lambda}_\ell$	$\eta_L = 1, \eta_R = 0$	$R_2^{5/3}$	$-y_{2\ 3j}^{RL}$	$t\ell$	100%

TABLE I. Summary of the four benchmark scenarios considered. They are explained in Section II A.

- 1. Left-handed Couplings Same Sign (LCSS):** In this scenario, we set  $\lambda_\ell = \lambda_\nu = \lambda$  and  $\eta_R = 0$ , i.e., we have a  $\phi_1$  LQ that couples to the left-handed leptons. As a result, the LQ couples to both  $t\ell$  and  $b\nu$  pairs with equal strength and hence decays to either of the pairs with about 50% BRs. In this scenario, the  $\phi_1$  behaves like the charge 1/3 component of  $S_3$  (with  $-y_{3\ 3j}^{LL} = \lambda$ ).
- 2. Left-handed Couplings Opposite Sign (LCOS):** We set  $\lambda_\ell = -\lambda_\nu = \lambda$  and  $\eta_R = 0$ . In this scenario too a  $\phi_1$  LQ couples with the left-handed leptons equally but with opposite signs. However, since it couples to both  $t\mu$  and  $b\nu$  pairs with equal (absolute) strength, it still decays to either  $t\ell$  or  $b\nu$  pairs with about 50% BRs. In this scenario, it behaves like an  $S_1$  with  $y_{1\ 3j}^{LL} = \lambda$  and  $y_{1\ 3j}^{RR} = 0$ .
- 3. Right-handed Coupling (RC):** In this scenario, the LQ has no weak charge and couples with only right handed leptons. This scenario is common to both  $\phi_1$  and  $\phi_5$  as we do not use the charge of leptoquark in our analysis. Here, we set  $\tilde{\lambda}_\ell = \lambda_\ell = \lambda$ ,  $\lambda_\nu = 0$  and  $\eta_L = 0$ . It decays to  $t\ell$  pair with 100% BR. In this scenario, the LQ is either of  $S_1$  type with  $y_{1\ 3j}^{LL} = 0$  and  $y_{1\ 3j}^{RR} = \lambda$  or it is  $R_2^{5/3}$  with  $y_{2\ j3}^{LR} = \lambda$ .
- 4. Left-handed Coupling (LC):** In this scenario the LQ couples with only left handed charged leptons. This scenario is exclusive  $\phi_5$ . Here, we set  $-y_{2\ 3j}^{RL} = \tilde{\lambda}_\ell = \lambda$  and  $\eta_R = 0$ . It decays to  $t\ell$  pair with 100% BR.

We have summarized these four scenarios in Table I.

### III. LHC PHENOMENOLOGY & SEARCH STRATEGY

We make use of various publicly available HEP packages for our collider analysis. We implement the effective Lagrangian of Eqs. (9) and (10) in FeynRules [44] to create the UFO [45] model files. Both signal and background events are generated in the event generator MadGraph5 [46] at the leading order (LO) and the higher-order corrections are included by multiplying appropriate QCD  $K$ -factors whenever available [47]. We use NNPDF2.3LO [48] parton distribution functions (PDFs) for event generation by setting default dynamical renormalisation and factorisation scales used in MadGraph5. Events are passed through Pythia6 [49] to perform showering and hadronization and matched up to two additional jets using MLM matching scheme [50, 51] with virtuality-ordered Pythia showers to remove the double counting of the matrix element partons with parton showers. Detector effects are simulated using Delphes3 [52] with the default CMS card. Fat-jets are reconstructed using FastJet [53] package by clustering Delphes tower objects. We employ Cambridge-Aachen [54] algorithm with ra-

dus parameter  $R = 1.5$  for fatjet clustering. To reconstruct hadronic top quark from fatjets, we use a popular top tagger, namely the HEPTopTagger [55].

#### A. Production at the LHC

As discussed in the Introduction, LQs are produced resonantly at the LHC through pair and single production channels. The LQ pair production is mostly model independent [depends only on the universal QCD coupling, see e.g. Fig. 1(a)] and proceeds through the  $gg$  and  $qq$  initiated processes. Note that in LCOS and LCSS models, the process  $bb \rightarrow \phi_1 \phi_1$  through the  $t$ -channel neutrino exchange is dependent on model coupling  $\lambda$  [see Fig. 1(b)]. However, this contribution is small in the total pair production cross section. The pair production process leads to the following final state,

$$pp \rightarrow \phi\phi \rightarrow (t\ell)(t\ell) \quad (11)$$

where a  $\phi$  stands for either a  $\phi_1$  or a  $\phi_5$ . Single production channels, where a LQ is produced in association with a lepton and either a jet or a top-quark, are given as,

$$\left. \begin{aligned} pp &\rightarrow \phi t\ell + \phi t\ell j \rightarrow (t\ell)t\ell + (t\ell)t\ell j \\ pp &\rightarrow \phi \ell j + \phi \ell j j \rightarrow (t\ell)\ell j + (t\ell)\ell j j \end{aligned} \right\} \quad (12)$$

In Fig. 2 we show the parton level cross sections of different production processes of  $\phi_1$  (a) and  $\phi_5$  (b) for new coupling  $\lambda = 1$ . We see that for  $\phi_1$ , the single productions depend heavily on whether it is an  $S_1$  with LCOS/RC type couplings or an  $S_3$  with LCSS coupling. In the LCSS scenario, the  $pp \rightarrow \phi_1 \ell j$  becomes the dominant process beyond  $M_\phi \gtrsim 1$  TeV whereas in the LCOS scenario, it overtakes the pair production only for  $M_\phi > 2.2$  TeV. This difference happens since in the LCOS scenario, some single production diagrams (see e.g. Figs. 1(c) & 1(d)) interfere destructively because of the opposite relative sign of the  $\lambda_\ell$  and  $\lambda_\nu$  couplings, whereas in case of LCSS, they interfere constructively. In the RC scenario, since a  $\phi_1$  does not couple to a  $b$ -quark or a left handed top quark (that can be produced from a  $W$  boson and a  $b$ -quark interaction),  $\sigma(pp \rightarrow \phi_1 \ell j)$  is expected not to be large. We see that  $\sigma(pp \rightarrow \phi_1 \ell j) < \sigma(pp \rightarrow \phi\phi)$  for  $M_\phi < 3$  TeV. For  $\phi_5$ , the cross section of  $pp \rightarrow \phi_5 \ell j$  processes is smaller in the RC scenario, as in this case the  $\phi_5$  couples exclusively to a right handed top quark.

It is clear from the cross section plots that for order one new coupling(s), it is important to consider single productions of LQs while estimating their discovery reach. Before we move on, we note that the cross section plots do not show the full picture, as one has to consider LQ branching ratios too. In the LCOS and LCSS scenarios the  $BR(\phi \rightarrow t\ell) \sim 50\%$  whereas it is 100% in RC and LC.

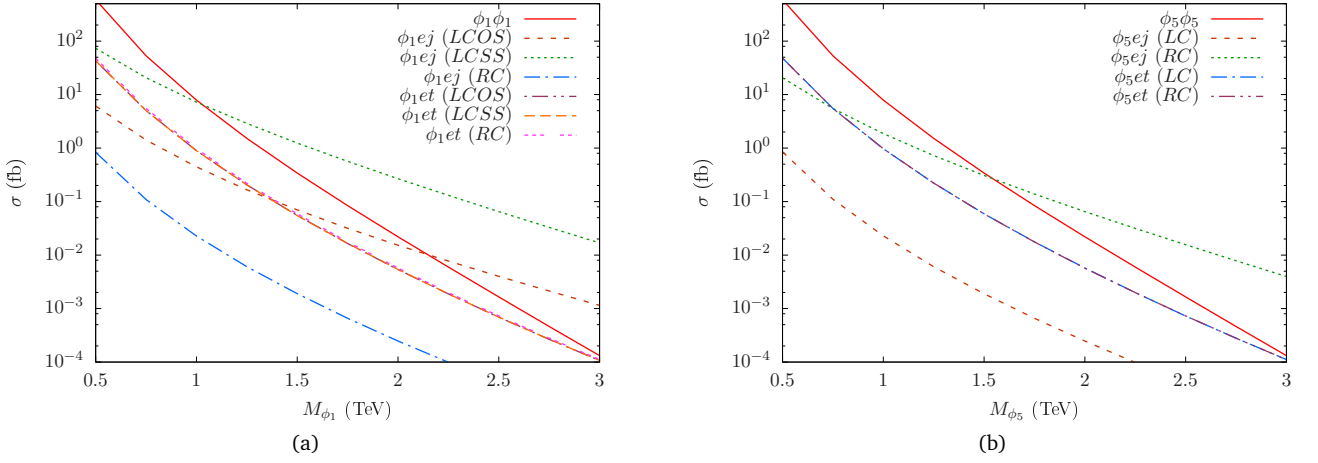


FIG. 2. The parton-level cross sections of different production channels of  $\phi_1$  and  $\phi_5$  at the 14 TeV LHC as functions of  $M_\phi$ . These cross sections are computed for a benchmark coupling  $\lambda = 1$  (see Table I). The pair production cross sections include an NLO QCD  $K$ -factor of 1.3 [47]. Here, the  $j$  in the single production processes includes all the light jets as well as  $b$ -jets. Their cross sections are generated with a cut on the transverse momentum of the jet,  $p_T^j > 20$  GeV.

### B. Signal Topology

In our analysis, we only consider the hadronic decays of tops so that we can reconstruct the top quark in the final states. The characteristic of our signal is one or two hadronically decaying boosted tops forming one/two top-like fatjets and two high- $p_T$  leptons. From Eqs. (11) and (12) we see that if we define the signal topology as events with *exactly two high- $p_T$  same flavour opposite sign (SFOS) leptons and at least one hadronic top-like fatjet in the final state* then it would include both single and pair productions and enhance the sensitivity.

There is some overlap between the pair and single production processes. For example, at the parton level, a  $t_h \ell t_h \ell$  final state can be produced from both pair production process as well as the  $pp \rightarrow \phi_1 t \ell$  process. Hence one has to be careful to avoid double counting while computing single productions [40]. In our simulations we achieve this by ensuring that for any single production process both  $\phi$  and  $\phi^\dagger$  are never on-shell simultaneously.

### C. The SM Backgrounds

The main SM background processes for this signal topology are those which contain two high- $p_T$  leptons and a top-like jet originating from an actual top quark or other jets (which can come from hadronic decays of the SM particles or from QCD jets) present in that process. Hence, the SM single  $Z$  production becomes the dominant background. The SM  $t\bar{t}$  process also contributes. Processes with large cross section containing single lepton can also act as a background if the second lepton appear due to a jet misidentified as a lepton. However, due to very small misidentification rate, these class of processes contribute negligibly to the total background.

Although some backgrounds are seemingly huge, events that would satisfy the final signal selection used in our analysis would actually come from a very specific kinematic region. For better statistics and saving computation time we generate all the large background processes with some strong generation level cuts.

#### Generation level cuts:

1.  $p_T(\ell_1) > 250$  GeV,

2. the invariant mass of the lepton pair  $M(\ell_1, \ell_2) > 115$  GeV (the  $Z$ -veto).

The last cut mainly controls the  $t\bar{t}$  background. Below, we discuss the different background processes in more detail.

#### 1. $V + jets$ :

Inclusive single vector boson ( $V = Z, W$ ) production processes in the SM have very large cross sections and therefore, can act as potential backgrounds for our signal even if the cut efficiencies are extremely small. There are two types of single vector boson processes that we consider as potential backgrounds.

- (a)  $Z + jets$ : This background is generated by simulating the process,  $pp \rightarrow Z + (0, 1, 2, 3)\text{-jets} \rightarrow \ell\ell + jets$  matched up to three extra partons. Here, the two high- $p_T$  leptons can arise from the leptonic decays of the  $Z$ -boson and a top-like fatjet can originate from the QCD jets. Since the invariant mass of the two leptons peaks at  $Z$ -mass, this background is controlled by applying a  $Z$ -mass veto.
- (b)  $W + jets$ : This process also has huge cross section like the previous one, but it is a reducible background. We generate it by simulating the process,  $pp \rightarrow W + (0, 1, 2, 3)\text{-jets} \rightarrow \ell\nu + jets$  matched up to three extra partons. Requirement of a top-like jet can be fulfilled if the QCD jets mimic as a top-jet. This is the only single lepton category potential background we have considered. However, as we demand the second lepton also to have high  $p_T$  where the lepton misidentification efficiency becomes small, we found this background to be negligible.

#### 2. $VV + jets$ :

There are four types of diboson processes viz.  $Z_\ell Z_h$ ,  $W_h Z_\ell$ ,  $W_\ell W_\ell$  and  $Z_\ell H_h$  that can act as sources of two high- $p_T$  leptons. The subscripts “ $\ell$ ” and “ $h$ ” represent leptonic and hadronic decay modes respectively. In these cases, the required top-like jet can arise from the hadronic decay products of bosons or from the QCD jets. Processes containing leptonically decaying  $Z$  can be drastically reduced by applying  $Z$  mass veto on the invariant mass of the lepton pair. We do not consider



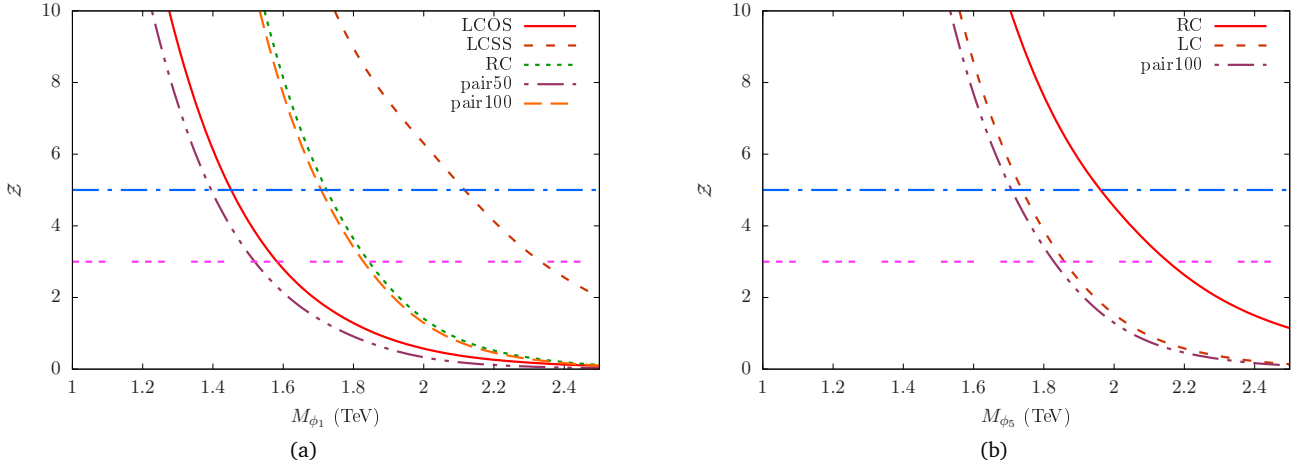


FIG. 3. Expected significances for (a)  $\phi_1$  and (b)  $\phi_2$  as functions of their masses for the  $3 \text{ ab}^{-1}$  integrated luminosity at the 14TeV LHC for different coupling scenarios. We use combined pair and single productions for the LCOS, LCSS, RC and LC scenarios. For comparison, we also show the pair production only significance for 50% (pair50) and 100% (pair100) BR to  $te$  mode. To estimate the single production,  $\lambda = 1$  is used. These plots are obtained using our event selection cuts defined in Section III D where we select events with at least one hadronically decaying boosted top and two high- $p_T$  opposite sign electrons.

the case where one lepton come from the vector boson decays and the other appear due to jets misidentified as leptons. We generate matched event samples including up to two jets of these processes.

### 3. $tt + jets$ :

The SM top pair production at the LHC can provide us two high- $p_T$  leptons when both the tops decay leptonically. Additionally, a top-like jet which arise from the QCD jets together with those two leptons can mimic our signal. We find that this background is the dominant one in our case. The  $t_\ell t_h$  process i.e. one top decays leptonically and the other hadronically can also contribute in our background. We generate this events by matching up to two additional jets.

### 4. $ttV$ :

The SM processes with a top pair associated with a vector boson can act as backgrounds for our signal. We consider the following four cases viz.  $t_\ell t_h Z_h$ ,  $t_\ell t_h W_h$ ,  $t_h t_h Z_\ell$ ,  $t_h t_h W_\ell$  depending on the decays of tops and vector bosons. We generate these event samples without adding extra jets in the final state.

### 5. $tW$ :

The SM  $pp \rightarrow t_\ell W_\ell$  process contains two leptons in the final state and contribute to the background for our signal. We generate this process using matching by adding up to two extra jets.

## D. Event selection

We apply the following sets of cuts on the signal and background events sequentially.

- $C_1$ : (a) At least one top-jet (obtained from HEPTopTagger) with  $p_T(t_h) > 135 \text{ GeV}$ .  
(b) Two SFOS with  $p_T(\ell_1) > 400 \text{ GeV}$  and  $p_T(\ell_2) > 200 \text{ GeV}$  (where  $\ell_1$  and  $\ell_2$  are  $p_T$ -ordered leptons) and pseudorapidity  $|\eta(\ell)| < 2.5$ . For electron we consider the barrel-endcap cut on  $\eta$  between 1.37 and 1.52.  
(c) Invariant mass of lepton pair  $M(\ell_1, \ell_2) > 120 \text{ GeV}$  to avoid  $Z$ -peak.  
(d) The missing energy  $\cancel{E}_T < 200 \text{ GeV}$ .

$C_2$ : The scalar sum of the transverse  $p_T$  of all visible objects,  $S_T > 1.2 \times \text{Min}(M_\phi, 1750) \text{ GeV}$ .

$C_3$ :  $M(\ell_1, t)$  OR  $M(\ell_2, t) > 0.8 \times \text{Min}(M_\phi, 1750) \text{ GeV}$ .

## E. Discovery potential

In Fig. 3, we show the expected significances for  $\phi_1$  and  $\phi_2$  LQs as functions of their masses for  $3 \text{ ab}^{-1}$  of integrated luminosity at the 14 TeV LHC with the benchmark coupling scenarios defined in Section II A. We have used the combined signal (includes pair and single production events) to estimate the reach for the LCOS, LCSS, RC and LC scenarios with  $\lambda = 1$ . For the LCOS and LCSS scenarios, the BR of LQ to  $te$  mode is 50% whereas for the RC and LC scenarios it is 100%. For comparison, we also show the expected significance for only the pair production (i.e.  $\lambda \rightarrow 0$ ) with 50% and 100% BR cases. Having computed the number of survived signal ( $N_S$ ) and background ( $N_B$ ) events by applying the selection cuts defined in Section III D, we estimate the expected significance ( $\mathcal{Z}$ ) by employing the following formula

$$\mathcal{Z} = \sqrt{2(N_S + N_B) \ln \left( \frac{N_S + N_B}{N_B} \right)} - 2N_S. \quad (13)$$

The CMS collaboration has performed the projected reach of pair production of LQ decaying into  $t\mu$  mode in Ref. [38]. With the 100% BR assumption in the  $t\mu$  mode, they have obtained a  $5\sigma$  discovery reach of LQ mass of about 1.8 TeV (considering statistical uncertainty only). Our estimation is quite close, about 1.75 TeV if we consider only pair production with 100% BR in the  $te$  mode. In the RC scenario for  $\phi_1$ , since the single production is very small compared to the pair production, the reach is almost identical to the pair production only reach. A similar situation is observed in the LC scenario for  $\phi_5$ . As explained in Section III, in both the RC scenario for  $\phi_1$  and the LC scenario for  $\phi_5$ , leptoquarks couple to the right-handed tops. As a result, single productions in these cases are suppressed as right-handed tops couple with charged current through chirality flipping.

The discovery reach for the pair production reduces with the reduction of BR of the  $te$  mode. For the LCOS and LCSS scenarios, the BR  $\phi_1 \rightarrow te$  is 50% and therefore, the  $5\sigma$  discovery reach for the pair production goes down to about 1.4 TeV. We observe a drastic enhancement of about 0.7 TeV in the discovery reach in the LCSS scenario as the  $pp \rightarrow \phi_1 e j$  cross section is large in the high mass region leading to a substantial number of events surviving the applied selection cuts. As explained earlier, in the LCSS scenario, the single production is large due to constructive interference whereas in the LCOS case the improvement is minor as the single production is small due to destructive interference. In case for  $\phi_5$ , the reaches are almost identical of about 1.75 TeV in pair-only and LC scenarios. But the reach goes up by about 0.2 TeV in the RC scenario.

#### IV. SUMMARY AND CONCLUSION

In this paper, we have studied the HL-LHC reach for discovering scalar LQs that decay to a top quark and a charged lepton. In particular, we have considered TeV-scale charge  $1/3$  ( $\phi_1$ ) and  $5/3$  ( $\phi_5$ ) scalar LQs that produce a boosted and hadronically decaying top quark and an electron. According to the classification given in Refs. [42, 43], only the  $S_1$ ,  $S_3$  (charge  $1/3$  component of the triplet) and  $R_2$  (charge  $5/3$  component of the doublet) scalar LQs can produce the specific signatures of our consideration. We have also introduced a simplified Lagrangian for  $\phi = \{\phi_1, \phi_5\}$  suitable for bottom-up searches. We have shown how these simplified models are connected to the actual models for different coupling configurations.

LQs can be produced in pairs ( $pp \rightarrow \phi\phi$ ) or singly  $pp \rightarrow \phi e j$ ,  $\phi e t$  at the LHC. We have observed that the  $pp \rightarrow \phi e j$  single production with order one couplings can overcome pair

production in certain coupling scenarios. For instance, in the LCSS scenario for  $\phi_1$  and the RC scenario for  $\phi_5$  (see Section II A), single production exceeds pair production in heavier mass region. We have employed a combined search strategy where the signal consists of from both pair and single production processes and demand at least one hadronically decaying boosted top and two opposite sign same flavour leptons. This selection criterion captures events from pair as well as single productions.

With this, we have found that the  $5\sigma$  discovery reach for  $\phi_1$  in LCSS scenario with  $\lambda = 1$  is about 2.1 TeV at the 14 TeV LHC with  $3 \text{ ab}^{-1}$  integrated luminosity. In the LCSS scenario, the BR  $\phi \rightarrow te$  mode is 50% and the reach for the pair production is only about 1.4 TeV. This significant improvement is due to constructive interference among certain single production diagrams. This increases the  $pp \rightarrow \phi e j$  cross section about one order in magnitude compared to the LCOS case where destructive interference makes single production unimportant. Finally we note that the enhancements of discovery reach due to the single production channels would increase further if the new couplings are more than one as the single production cross sections scale as square of the coupling involved.

#### ACKNOWLEDGMENTS

T.M. is grateful to the Royal Society of Arts and Sciences of Uppsala for financial support as a guest researcher at Uppsala University during the initial stage of this project. S.M. acknowledges support from the Science and Engineering Research Board (SERB), DST, India under grant number ECR/2017/000517. We thank R. Arvind Bhaskar for reading and commenting on the manuscript.

- 
- [1] **BaBar** collaboration, J. P. Lees et al., *Evidence for an excess of  $\bar{B} \rightarrow D^{(*)}\tau^-\bar{\nu}_\tau$  decays*, *Phys. Rev. Lett.* **109** (2012) 101802, [1205.5442].
  - [2] **BaBar** collaboration, J. P. Lees et al., *Measurement of an Excess of  $\bar{B} \rightarrow D^{(*)}\tau^-\bar{\nu}_\tau$  Decays and Implications for Charged Higgs Bosons*, *Phys. Rev.* **D88** (2013) 072012, [1303.0571].
  - [3] **LHCb** collaboration, R. Aaij et al., *Measurement of the ratio of branching fractions  $\mathcal{B}(\bar{B}^0 \rightarrow D^{*+}\tau^-\bar{\nu}_\tau)/\mathcal{B}(\bar{B}^0 \rightarrow D^{*+}\mu^-\bar{\nu}_\mu)$* , *Phys. Rev. Lett.* **115** (2015) 111803, [1506.08614]. [Erratum: *Phys. Rev. Lett.* 115, no. 15, 159901 (2015)].
  - [4] **LHCb** collaboration, R. Aaij et al., *Measurement of the ratio of the  $B^0 \rightarrow D^{*-}\tau^+\nu_\tau$  and  $B^0 \rightarrow D^{*-}\mu^+\nu_\mu$  branching fractions using three-prong  $\tau$ -lepton decays*, *Phys. Rev. Lett.* **120** (2018) 171802, [1708.08856].
  - [5] **LHCb** collaboration, R. Aaij et al., *Test of Lepton Flavor Universality by the measurement of the  $B^0 \rightarrow D^{*-}\tau^+\nu_\tau$  branching fraction using three-prong  $\tau$  decays*, *Phys. Rev.* **D97** (2018) 072013, [1711.02505].
  - [6] **Belle** collaboration, S. Hirose et al., *Measurement of the  $\tau$  lepton polarization and  $R(D^*)$  in the decay  $\bar{B} \rightarrow D^{*+}\tau^-\bar{\nu}_\tau$* , *Phys. Rev. Lett.* **118** (2017) 211801, [1612.00529].
  - [7] **Belle** collaboration, S. Hirose et al., *Measurement of the  $\tau$  lepton polarization and  $R(D^*)$  in the decay  $\bar{B} \rightarrow D^{*+}\tau^-\bar{\nu}_\tau$  with one-prong hadronic  $\tau$  decays at Belle*, *Phys. Rev.* **D97** (2018) 012004, [1709.00129].
  - [8] **Belle** collaboration, A. Abdesselam et al., *Measurement of  $R(D)$  and  $R(D^*)$  with a semileptonic tagging method*, 1904.08794.
  - [9] **HFLAV** collaboration, Y. Amhis et al., *Averages of  $b$ -hadron,  $c$ -hadron, and  $\tau$ -lepton properties as of summer 2016*, *Eur. Phys. J.* **C77** (2017) 895, [1612.07233]. We have used the Spring 2019 averages from <https://hflav-eos.web.cern.ch/hflav-eos/semi/spring19/htm>. For regular updates see <https://hflav.web.cern.ch/content/semileptonic-b-decays>.
  - [10] D. Bigi and P. Gambino, *Revisiting  $B \rightarrow D\ell\nu$* , *Phys. Rev.* **D94** (2016) 094008, [1606.08030].
  - [11] F. U. Bernlochner, Z. Ligeti, M. Papucci and D. J. Robinson, *Combined analysis of semileptonic  $B$  decays to  $D$  and  $D^*$ :  $R(D^{(*)})$ ,  $|V_{cb}|$ , and new physics*, *Phys. Rev.* **D95** (2017) 115008, [1703.05330]. [erratum: *Phys. Rev.* D97, no. 5, 059902 (2018)].
  - [12] D. Bigi, P. Gambino and S. Schacht,  *$R(D^*)$ ,  $|V_{cb}|$ , and the Heavy Quark Symmetry relations between form factors*, *JHEP* **11** (2017) 061, [1707.09509].
  - [13] S. Jaiswal, S. Nandi and S. K. Patra, *Extraction of  $|V_{cb}|$  from  $B \rightarrow D^{(*)}\ell\nu_\ell$  and the Standard Model predictions of  $R(D^{(*)})$* , *JHEP* **12** (2017) 060, [1707.09977].
  - [14] G. Hiller and F. Kruger, *More model-independent analysis of  $b \rightarrow s$  processes*, *Phys. Rev.* **D69** (2004) 074020, [hep-ph/0310219].

- [15] M. Bordone, G. Isidori and A. Pattori, *On the Standard Model predictions for  $R_K$  and  $R_{K^*}$* , *Eur. Phys. J. C* **76** (2016) 440, [[1605.07633](#)].
- [16] LHCb collaboration, R. Aaij et al., *Test of lepton universality using  $B^+ \rightarrow K^+ \ell^+ \ell^-$  decays*, *Phys. Rev. Lett.* **113** (2014) 151601, [[1406.6482](#)].
- [17] LHCb collaboration, R. Aaij et al., *Differential branching fractions and isospin asymmetries of  $B \rightarrow K^{(*)} \mu^+ \mu^-$  decays*, *JHEP* **06** (2014) 133, [[1403.8044](#)].
- [18] LHCb collaboration, R. Aaij et al., *Angular analysis of the  $B^0 \rightarrow K^{*0} \mu^+ \mu^-$  decay using  $3 \text{ fb}^{-1}$  of integrated luminosity*, *JHEP* **02** (2016) 104, [[1512.04442](#)].
- [19] LHCb collaboration, R. Aaij et al., *Test of lepton universality with  $B^0 \rightarrow K^{*0} \ell^+ \ell^-$  decays*, *JHEP* **08** (2017) 055, [[1705.05802](#)].
- [20] LHCb collaboration, R. Aaij et al., *Search for lepton-universality violation in  $B^+ \rightarrow K^+ \ell^+ \ell^-$  decays*, *Phys. Rev. Lett.* **122** (2019) 191801, [[1903.09252](#)].
- [21] J. C. Pati and A. Salam, *Lepton Number as the Fourth Color*, *Phys. Rev. D* **10** (1974) 275–289. [Erratum: *Phys. Rev. D* **11**, 703 (1975)].
- [22] H. Georgi and S. L. Glashow, *Unity of All Elementary Particle Forces*, *Phys. Rev. Lett.* **32** (1974) 438–441.
- [23] B. Schrempp and F. Schrempp, *Light Leptoquarks*, *Phys. Lett. B* **153** (1985) 101–107.
- [24] R. Barbier et al., *R-parity violating supersymmetry*, *Phys. Rept.* **420** (2005) 1–202, [[hep-ph/0406039](#)].
- [25] M. Kohda, H. Sugiyama and K. Tsumura, *Lepton number violation at the LHC with leptoquark and diquark*, *Phys. Lett. B* **718** (2013) 1436–1440, [[1210.5622](#)].
- [26] J. M. Arnold, B. Fornal and M. B. Wise, *Phenomenology of scalar leptoquarks*, *Phys. Rev. D* **88** (2013) 035009, [[1304.6119](#)].
- [27] P. Bandyopadhyay and R. Mandal, *Revisiting scalar leptoquark at the LHC*, *Eur. Phys. J. C* **78** (2018) 491, [[1801.04253](#)].
- [28] N. Vignaroli, *Seeking leptoquarks in the  $t\bar{t}$  plus missing energy channel at the high-luminosity LHC*, *Phys. Rev. D* **99** (2019) 035021, [[1808.10309](#)].
- [29] T. Mandal, S. Mitra and S. Raz,  *$R_{D^{(*)}}$  in minimal leptoquark scenarios: impact of interference on the exclusion limits from LHC data*, [[1811.03561](#)].
- [30] U. Aydemir, T. Mandal and S. Mitra, *A single TeV-scale scalar leptoquark in  $\text{SO}(10)$  grand unification and B-decay anomalies*, [[1902.08108](#)].
- [31] CMS collaboration, A. M. Sirunyan et al., *Search for third-generation scalar leptoquarks decaying to a top quark and a  $\tau$  lepton at  $\sqrt{s} = 13 \text{ TeV}$* , *Eur. Phys. J. C* **78** (2018) 707, [[1803.02864](#)].
- [32] CMS collaboration, A. M. Sirunyan et al., *Constraints on models of scalar and vector leptoquarks decaying to a quark and a neutrino at  $\sqrt{s} = 13 \text{ TeV}$* , *Phys. Rev. D* **98** (2018) 032005, [[1805.10228](#)].
- [33] ATLAS collaboration, M. Aaboud et al., *Searches for scalar leptoquarks and differential cross-section measurements in dilepton-dijet events in proton-proton collisions at a centre-of-mass energy of  $\sqrt{s} = 13 \text{ TeV}$  with the ATLAS experiment*, [[1902.00377](#)].
- [34] ATLAS collaboration, M. Aaboud et al., *Searches for third-generation scalar leptoquarks in  $\sqrt{s} = 13 \text{ TeV}$  pp collisions with the ATLAS detector*, [[1902.08103](#)].
- [35] B. Diaz, M. Schmaltz and Y.-M. Zhong, *The leptoquark Hunter’s guide: Pair production*, *JHEP* **10** (2017) 097, [[1706.05033](#)].
- [36] M. Schmaltz and Y.-M. Zhong, *The leptoquark Hunter’s guide: large coupling*, *JHEP* **01** (2019) 132, [[1810.10017](#)].
- [37] CMS collaboration, A. M. Sirunyan et al., *Search for leptoquarks coupled to third-generation quarks in proton-proton collisions at  $\sqrt{s} = 13 \text{ TeV}$* , *Phys. Rev. Lett.* **121** (2018) 241802, [[1809.05558](#)].
- [38] CMS collaboration, *Projection of searches for pair production of scalar leptoquarks decaying to a top quark and a charged lepton at the HL-LHC*, Tech. Rep. CMS-PAS-FTR-18-008, 2018.
- [39] T. Mandal and S. Mitra, *Probing Color Octet Electrons at the LHC*, *Phys. Rev. D* **87** (2013) 095008, [[1211.6394](#)].
- [40] T. Mandal, S. Mitra and S. Seth, *Single Productions of Colored Particles at the LHC: An Example with Scalar Leptoquarks*, *JHEP* **07** (2015) 028, [[1503.04689](#)].
- [41] T. Mandal, S. Mitra and S. Seth, *Probing Compositeness with the CMS  $eejj$  &  $eej$  Data*, *Phys. Lett. B* **758** (2016) 219–225, [[1602.01273](#)].
- [42] W. Buchmuller, R. Ruckl and D. Wyler, *Leptoquarks in Lepton - Quark Collisions*, *Phys. Lett. B* **191** (1987) 442–448. [Erratum: *Phys. Lett. B* **448**, 320 (1999)].
- [43] I. Doršner, S. Fajfer, A. Greljo, J. F. Kamenik and N. Košnik, *Physics of leptoquarks in precision experiments and at particle colliders*, *Phys. Rept.* **641** (2016) 1–68, [[1603.04993](#)].
- [44] A. Alloul, N. D. Christensen, C. Degrande, C. Duhr and B. Fuks, *FeynRules 2.0 - A complete toolbox for tree-level phenomenology*, *Comput. Phys. Commun.* **185** (2014) 2250–2300, [[1310.1921](#)].
- [45] C. Degrande, C. Duhr, B. Fuks, D. Grellscheid, O. Mattelaer and T. Reiter, *UFO - The Universal FeynRules Output*, *Comput. Phys. Commun.* **183** (2012) 1201–1214, [[1108.2040](#)].
- [46] J. Alwall, R. Frederix, S. Frixione, V. Hirschi, F. Maltoni, O. Mattelaer et al., *The automated computation of tree-level and next-to-leading order differential cross sections, and their matching to parton shower simulations*, *JHEP* **07** (2014) 079, [[1405.0301](#)].
- [47] T. Mandal, S. Mitra and S. Seth, *Pair Production of Scalar Leptoquarks at the LHC to NLO Parton Shower Accuracy*, *Phys. Rev. D* **93** (2016) 035018, [[1506.07369](#)].
- [48] R. D. Ball et al., *Parton distributions with LHC data*, *Nucl. Phys. B* **867** (2013) 244–289, [[1207.1303](#)].
- [49] T. Sjostrand, S. Mrenna and P. Z. Skands, *PYTHIA 6.4 Physics and Manual*, *JHEP* **05** (2006) 026, [[hep-ph/0603175](#)].
- [50] M. L. Mangano, M. Moretti, F. Piccinini and M. Treccani, *Matching matrix elements and shower evolution for top-quark production in hadronic collisions*, *JHEP* **01** (2007) 013, [[hep-ph/0611129](#)].
- [51] S. Hoeche, F. Krauss, N. Lavesson, L. Lonnblad, M. Mangano, A. Schalick et al., *Matching parton showers and matrix elements, in HERA and the LHC: A Workshop on the implications of HERA for LHC physics: Proceedings Part A*, 2006. [[hep-ph/0602031](#)].
- [52] DELPHES 3 collaboration, J. de Favereau, C. Delaere, P. Demin, A. Giammanco, V. Lemaitre, A. Mertens et al., *DELPHES 3, A modular framework for fast simulation of a generic collider experiment*, *JHEP* **02** (2014) 057, [[1307.6346](#)].
- [53] M. Cacciari, G. P. Salam and G. Soyez, *FastJet User Manual*, *Eur. Phys. J. C* **72** (2012) 1896, [[1111.6097](#)].

- [54] Y. L. Dokshitzer, G. D. Leder, S. Moretti and B. R. Webber, *Better jet clustering algorithms*, *JHEP* **08** (1997) 001, [[hep-ph/9707323](#)].
- [55] T. Plehn, M. Spannowsky, M. Takeuchi and D. Zerwas, *Stop Reconstruction with Tagged Tops*, *JHEP* **10** (2010) 078, [[1006.2833](#)].